Extreme Mechanics Letters 4 (2015) 156–161

Contents lists available at ScienceDirect

Extreme Mechanics Letters

journal homepage: www.elsevier.com/locate/eml

Influence of stiffening on elastic wave propagation in extremely deformed soft matter: from nearly incompressible to auxetic materials

Pavel I. Galich, Stephan Rudykh *

Department of Aerospace Engineering, Technion - Israel Institute of Technology, Haifa 32000, Israel

ARTICLE INFO

Article history:
Received 5 April 2015
Received in revised form 9 June 2015
Accepted 10 June 2015
Available online 14 June 2015

Keywords:
Elastic waves
Finite deformations
Soft materials
Compressible materials
Stiffening
Auxetics

ABSTRACT

We analyse the propagation of elastic waves in soft materials subjected to finite deformations. We derive explicit phase velocity relations for matter with pronounced stiffening effect, namely Gent model, and apply these results to study elastic wave propagation in (a) nearly incompressible materials such as biological tissues and polymers, (b) highly compressible and (c) negative Poisson's ratio or auxetic materials. We find, that for nearly incompressible materials transverse wave velocities exhibit strong dependence on the direction of propagation and initial strain state, whereas the longitudinal wave velocity is not affected significantly until extreme levels of deformation are attained. For highly compressible materials, we show that both longitudinal and transversal wave velocities depend strongly on deformation and direction of propagation. Moreover, the dependence becomes stronger when stiffening effects increase. When compression is applied, the longitudinal wave velocity decreases regardless the direction of wave propagation in highly compressible materials, and increases for most of the directions in materials with negative Poisson's ratio behaviour. We demonstrate that finite deformations can influence elastic wave propagation through combinations of induced effective compressibility and stiffness.

1. Introduction

The propagation of elastic waves has been investigated intensively [1–16] because the understanding of the phenomenon is vital for a large variety of applications from non-invasive material testing and medical imaging for health care to petroleum exploration. Recently, the field of acoustic or phononic metamaterials has attracted considerable attention. The peculiarity of these metamaterials originates in their microstructure [17,18], which can be tailored to give rise to various effects such as local resonances [19], band-gaps [12] and cloaking [20]. Furthermore, *soft* metamaterials, due to their capability to sustain large deformations, open promising opportunities of manipulating acoustic characteristics via deformation [21–23].

In this work, we derive explicit phase velocity relations for *finitely deformed* materials, which stiffen when stretched/compressed. Our analysis is based on the theory first developed by Hadamard [2], which was recently revised by Destrade and Ogden [11]. We specify the theory for the class of Gent materials, and obtain compact explicit expressions of phase velocities for any finite deformation and direction of propagation. The availability of explicit relations for phase velocity is important for designing *mechanotunable* acoustic metamaterials. Moreover, the information may benefit non-invasive medical diagnostic techniques by providing important information on the dependence of elastic wave propagation on pre-stress/pre-strain conditions, which are common in biological

* Corresponding author.
E-mail address: rudykh@technion.ac.il (S. Rudykh).

http://dx.doi.org/10.1016/j.eml.2015.06.003
2352-4316/

tissues. By application of the derived explicit expressions, we show the role of deformation and significant influence of stiffening effects on wave propagation in soft media undergoing finite deformations. Moreover, we extend the analysis to a class of exotic metamaterials characterized by negative Poisson's ratio (NPR) behaviour. Examples of NPR materials, also known as *auxetics*, include living bone tissue [24], skin [25], blood vessels [26], certain rocks and minerals [25], and artificial materials [27]. As we shall show, elastic wave propagation in these materials is significantly affected by deformation. In our analysis, we treat the materials as continuous media; their overall homogenized behaviour is characterized by effective elastic moduli. These material properties may originate in sophisticatedly engineered microstructures that give rise to remarkable overall properties (for example, negative Poisson's ratio or/and bulk modulus). The information on elastic wave propagation in terms of the effective properties can guide the design of new tunable metamaterials. Moreover, this information can shed light on the distinct roles of geometrical changes and material non-linearities occurring in tunable metamaterials due to large deformations [28]. Furthermore, even simple homogeneous materials can behave like smart metamaterials when finitely deformed. For example, they can be used to disentangle shear and pressure waves [23,29].

2. Analysis

To analyse the finitely deformed state, we introduce the deformation gradient $\mathbf{F}(\mathbf{X},t) = \nabla_{\mathbf{X}} \otimes \mathbf{x}(\mathbf{X},t)$, where $\mathbf{X}$ and $\mathbf{x}$ are position vectors in the reference and current configurations, respectively. To take into account the non-linear effects of the finite deformation as well as material non-linearity, we analyse the wave propagation in terms of infinitesimal plane waves *superimposed* on a finitely deformed state [2,4]. To account for the stiffening effects (due to, for example, finite extensibility of polymer chains, or due to collective straightening of collagen fibres in biological tissues) in finitely deformed media, we make use of the strain–energy density function corresponding to an approximation of the Arruda–Boyce model [30], namely the Gent model [31,32] which is given in Eq. (1).

$$\psi(\mathbf{F}) = -\frac{\mu J_m}{2}\ln\left(1-\frac{I_1-3}{J_m}\right) - \mu\ln J + \left(\frac{K}{2}-\frac{\mu}{3}-\frac{\mu}{J_m}\right)(J-1)^2, \quad (1)$$

where μ is the initial shear modulus, K is the initial bulk modulus, $I_1 = \operatorname{tr}\mathbf{B}$ is the first invariant of the left Cauchy–Green tensor $\mathbf{B} = \mathbf{F}\cdot\mathbf{F}^T$, and $J = \det \mathbf{F}$. The model neatly covers the stiffening of the material with the deformation; as the first strain invariant approaches $I_1 = 3 + J_m$, the energy function becomes unbounded and a dramatic increase in stress occurs. Consequently, J_m is a locking parameter. Clearly, when $J_m \to \infty$, the strain–energy function (1) reduces to

$$\psi(\mathbf{F}) = \frac{\mu}{2}(I_1-3) - \mu\ln J + (K/2-\mu/3)(J-1)^2, \quad (2)$$

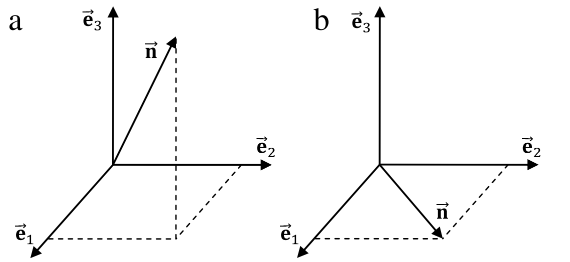

Fig. 1. Direction of propagation $\mathbf{n}$ relating to principal directions in general case (a) and when $\mathbf{n}$ lies in one of the planes of orthotropy (b). Here $(\mathbf{e}_1, \mathbf{e}_2, \mathbf{e}_3)$ is orthonormal basis of eigenvectors of left Cauchy–Green tensor $\mathbf{B}$.

which is a compressible extension of the neo-Hookean strain–energy function [33].

Recall the definition of an acoustic tensor [2,4] which defines the condition of propagation of plane waves

$$\mathbf{Q}(\mathbf{n}) = \mathcal{A}^{(1324)} : \mathbf{n}\otimes\mathbf{n}, \quad (3)$$

where the unit vector $\mathbf{n}$ defines the direction of propagation of the wave; $\mathcal{A} = J^{-1}\left(\mathbf{F}\cdot\mathcal{A}_0^{(2134)}\right)^{(2134)}\cdot\mathbf{F}^T$ and $\mathcal{A}_0 = \frac{\partial^2\psi}{\partial\mathbf{F}\partial\mathbf{F}}$ are tensors of elastic moduli in current and reference configuration respectively; superscripts (1324) and (2134) denote isomers of the fourth-rank tensors [34,35], as detailed in Appendix A.

Strong stiffening. Acoustic tensor for finitely deformed Gent material (1) takes the form

$$\mathbf{Q}(\mathbf{n}) = \frac{\mu}{J}\left(1+\left(\frac{K}{\mu}-\frac{2}{3}-\frac{2}{J_m}\right)J^2\right)\mathbf{n}\otimes\mathbf{n} + \frac{\mu J_m}{J\xi^2}\left(\xi(\mathbf{n}\cdot\mathbf{B}\cdot\mathbf{n})\mathbf{I} + 2\mathbf{n}\otimes\mathbf{n}:\mathbf{B}\otimes\mathbf{B}^{(1324)}\right), \quad (4)$$

where $\xi = 3+J_m-I_1$, $\mathbf{I}$ is the identity tensor, and $\mathbf{B}\otimes\mathbf{B}^{(1324)}$ is the fourth-rank tensor isomer (see Appendices A and B).

General case. One can conclude from (4) that in general case (when $\mathbf{n}$ does not lie in any plane of orthotropy (Fig. 1(a)) and deformations are different along each principal axis, i.e. all eigenvalues of tensor $\mathbf{B}$ are different) the waves are neither purely longitudinal nor purely transversal (for details see Appendix B).

Case 1. If wave vector $\mathbf{n}$ lies in one of the planes of orthotropy (Fig. 1(b)) then we always have one purely transversal wave with the velocity

$$c_{tr} = \sqrt{\mu(\mathbf{n}\cdot\mathbf{B}\cdot\mathbf{n})J_m/(\rho_0\xi)}, \quad (5)$$

where ρ_0 is the density of the undeformed material. Any finite deformation $\mathbf{F}$ at a homogeneous state can be represented as

$$\mathbf{F} = \lambda_1\mathbf{e}_1\otimes\mathbf{e}_1 + \lambda_2\mathbf{e}_2\otimes\mathbf{e}_2 + \lambda_3\mathbf{e}_3\otimes\mathbf{e}_3, \quad (6)$$

where $\lambda_{1,2,3}$ are stretch ratios along principal directions. Thus, expression (5) holds true for any combination of λ_1, λ_2 and λ_3.

Case 2. When wave vector $\mathbf{n}$ lies in one of the planes of orthotropy (for example in $\mathbf{e}_1 - \mathbf{e}_2$) and stretch ratios in this plane are equal ($\lambda_1 = \lambda_2 = \hat{\lambda}$) then we have one longitudinal and two transversal polarizations with following velocities

$$c_l = \sqrt{\mu\left(1+\eta J^2 + J_m\xi^{-2}\left(\xi + 2\hat{\lambda}^2\right)\hat{\lambda}^2\right)/\rho_0} \tag{7}$$

and

$$c_{tr} = \hat{\lambda}\sqrt{\mu J_m/(\rho_0\xi)} \tag{8}$$

respectively, with $\eta = K/\mu - 2/3 - 2/J_m$.

Case 3. For waves propagating along the principal direction ($\mathbf{n} = \mathbf{e}_i$), the velocities of longitudinal and transversal waves are

$$c_l = \sqrt{\mu\left(1+\eta J^2 + J_m\xi^{-2}\left(\xi + 2\lambda_i^2\right)\lambda_i^2\right)/\rho_0} \tag{9}$$

and

$$c_{tr} = \lambda_i\sqrt{\mu J_m/(\rho_0\xi)}. \tag{10}$$

Case 4. When materials undergo so-called uniform dilatation or compaction ($\lambda_1 = \lambda_2 = \lambda_3$ or $\mathbf{F} = q\mathbf{I}$), then we have only pure modes with the velocities given by

$$c_l = \sqrt{\mu\left(1+\left(\eta q^4 + J_m\xi^{-2}\left(\xi + 2q^2\right)\right)q^2\right)/\rho_0} \tag{11}$$

and

$$c_{tr} = q\sqrt{\mu J_m/(\rho_0\xi)}. \tag{12}$$

Weak stiffening. In case of a weak stiffening effect, namely, $J_m \to \infty$, the acoustic tensor (4) reduces to the well-known expression [9]

$$\mathbf{Q}(\mathbf{n}) = a_1\mathbf{n}\otimes\mathbf{n} + a_2(\mathbf{I} - \mathbf{n}\otimes\mathbf{n}), \tag{13}$$

where $\mathbf{n}\otimes\mathbf{n}$ is the projection on the direction $\mathbf{n}$; $(\mathbf{I}-\mathbf{n}\otimes\mathbf{n})$ is the projection on the plane normal to $\mathbf{n}$; $a_1 = (K - 2\mu/3)J + \mu J^{-1}(1 + \mathbf{n}\cdot\mathbf{B}\cdot\mathbf{n})$ and $a_2 = \mu J^{-1}(\mathbf{n}\cdot\mathbf{B}\cdot\mathbf{n})$. Consequently, there always exist one longitudinal and two transverse waves for any direction of propagation $\mathbf{n}$. Phase velocities of these waves can be calculated as [13] $c_l = \sqrt{a_1 J/\rho_0}$ and $c_{tr} = \sqrt{a_2 J/\rho_0}$. In the small deformation limit these formulae reduce to $c_l = \sqrt{(K + 4\mu/3)/\rho_0}$ and $c_{tr} = \sqrt{\mu/\rho_0}$. It is worth mentioning that Boulanger and Hayes [13,16] presented explicit phase velocity expressions for wide classes of Hadamard and Mooney–Rivlin materials; however, the Gent material model, considered here, does not belong to these classes of hyperelastic materials.

3. Examples

To illustrate the dependence of wave propagation on the deformation and direction of propagation, we consider the case of uniaxial tension

$$\mathbf{F} = \lambda\mathbf{e}_1\otimes\mathbf{e}_1 + \tilde{\lambda}(\mathbf{I} - \mathbf{e}_1\otimes\mathbf{e}_1), \tag{14}$$

where λ is the applied stretch ratio and $\tilde{\lambda} = \tilde{\lambda}(\lambda, K/\mu)$ is defined through λ and the compressibility of the material. Remind that the compressibility of the material is defined by the ratio K/μ. In the linear elastic limit the elastic moduli are related through

$$\frac{K}{\mu} = \frac{2(1+\nu)}{3(1-2\nu)}, \tag{15}$$

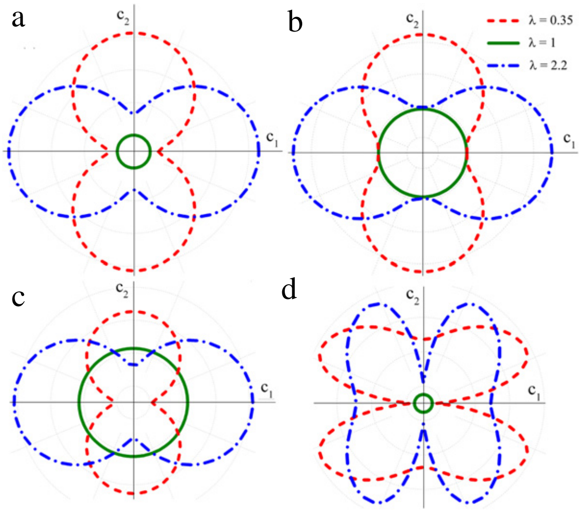

Fig. 2. Polar diagrams of the phase velocities in nearly incompressible materials: for the purely transversal (a), quasi-longitudinal (b), quasi-transversal (d) waves in Gent material with $J_m = 3$ and $K/\mu = 300$; and for the purely transversal (c) wave in neo-Hookean material with $K/\mu = 300$.

where ν is Poisson's ratio. Thus, $-1/3 < K/\mu < \infty$ with $\mu > 0$. Note that for $-1/3 < K/\mu < 0$ the material is stable only if constrained [34,36,37]. It follows from (15) that matter exhibits auxetic behaviour when $-1/3 < K/\mu < 2/3$.

Nearly incompressible materials. For nearly incompressible materials ($K/\mu \gg 1$ and $\tilde{\lambda} \simeq \lambda^{-1/2}$) the dependence of the longitudinal wave velocity on the direction of propagation and initial stress state is relatively weak unless extreme levels of deformation are attained. Fig. 2 shows the polar diagrams of the phase velocities for the nearly incompressible Gent and neo-Hookean materials under extreme levels of deformation. Here and thereafter the velocities are normalized by their value in the undeformed state; c_1 and c_2 are phase velocities along principal directions $\mathbf{e}_1$ and $\mathbf{e}_2$, correspondingly; more details on phase velocity or slowness surfaces can be found in the textbooks of Auld [38] or Nayfeh [39]. At the extreme levels of deformations, the stiffening effect manifests in a significant increase of the effective shear modulus, which becomes comparable with the bulk modulus (see Eq. (9)). Fig. 2(b) shows that velocity of longitudinal wave increases in both compressed and stretched materials. Moreover, stiffening of the material gives rise to the dramatic dependence of transversal wave velocities on the direction of propagation and deformation as compared to the materials with weak stiffening effect (compare Fig. 2(a) and (d) vs (c)). Besides, we observe that the dependence of the phase velocities on deformation and propagation direction increases when the locking parameter J_m decreases (which corresponds to an earlier stiffening of the material with deformation). Comparing the quasi-transversal wave velocity profiles with the purely transversal ones on the Fig. 2, we observe that the velocity of quasi-transversal wave has maxima for the non-principal directions (Fig. 2(d)). Note

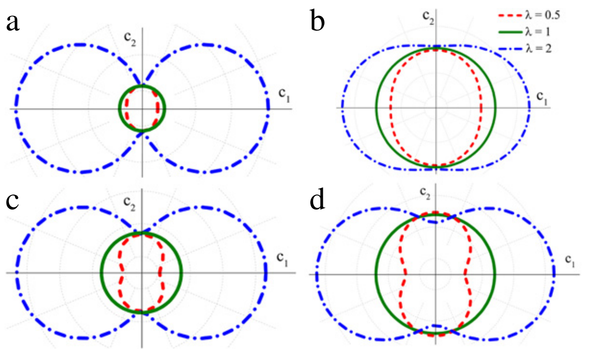

Fig. 3. Polar diagrams of the phase velocities in highly compressible materials: for the quasi-longitudinal (a) and purely transversal (c) waves in Gent material with $J_m = 3$ and $K/\mu = 1$; for the purely longitudinal (b) and transversal (d) waves in neo-Hookean material with $K/\mu = 1$.

that this phenomenon is not observed in Hadamard materials [40,41].

Highly compressible materials. In contrast to nearly incompressible materials, for highly compressible matter, the velocity of longitudinal wave depends strongly on the direction of propagation and initial deformation state even for moderate levels of deformation. More specifically Fig. 3(a) and (b) show that the velocity of pressure wave increases when material is stretched and decreases when it is compressed. Propagation of shear waves in highly compressible media differs significantly from the one in nearly incompressible materials. In particular, under compression the velocities of shear waves decrease in any direction if $K/\mu \leq 1$ (Fig. 3(c)), while it can either decrease or increase depending on the propagation direction in the nearly incompressible case (Fig. 2(a) and (c)). It should be noted that the deformation induced stiffening has a significant influence on both modes (compare Fig. 3(a), (c) vs (b), (d)), in particular when material is stretched. This is due to an increase in the effective shear modulus (the term $\mu J_m/\xi^2$ in Eq. (9) and $\mu J_m/\xi$ in Eq. (10)). The polar diagram of the phase velocity for the quasi-transversal wave in Gent material with $J_m = 3$ and $K/\mu = 1$ is similar to one plotted in Fig. 3(c), and it is not presented here.

Auxetic materials. Next, we consider auxetic materials characterized by NPR behaviour. Yet can such materials exist? Would they be stable? How can they be constructed? These questions have recently arisen in many papers [19,27,36,37,42–45] and still the topic is open for discussion. Wang and Lakes in their article [36] report that bulk modulus can be varied within the range $-\frac{4\mu}{3} < K < \infty$. Based on this and the previous estimations (Eq. (15)), we examine the material behaviour when $-1/3 < K/\mu < 0$. To illustrate the auxetic materials behaviour, we present the dependence of $\tilde{\lambda}$ and Poisson's ratio on the applied stretch λ for different ratios of K/μ.

Fig. 4 show that NPR behaviour is more pronounced in materials with negative bulk modulus. Note that the material becomes locally non-auxetic when certain level of deformation is reached. Furthermore, this level depends on stiffening of the material. In particular, materials with pronounced stiffening effect become locally non-auxetic faster than materials with weak stiffening effect. For

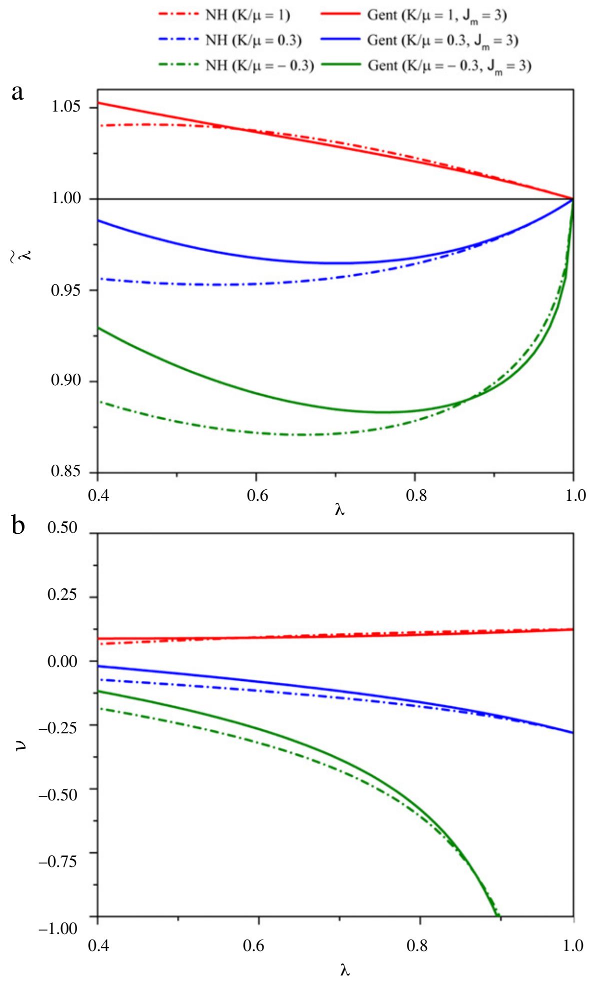

Fig. 4. Dependence of $\tilde{\lambda}$ (a) and Poisson's ratio ν (b) on applied stretch λ for Gent and neo-Hookean materials with different ratios K/μ.

example, $\lambda_{cr} \approx 0.66$ for neo-Hookean material with $K/\mu = -0.3$, and $\lambda_{cr} \approx 0.76$ for Gent material with $K/\mu = -0.3$ and $J_m = 3$.

An example of wave velocities for auxetic materials is shown in Fig. 5. We observe that the velocity of the longitudinal wave increases in any direction of propagation **n** when the material undergoes compression (Fig. 5(b)). This is in contrast to the case of highly compressible matter (see Fig. 3(a) and (b)). Moreover, the velocity of the longitudinal wave increases and reaches the maximum when wave vector **n** lies in the plane of transverse isotropy. However, for materials with strong stiffening effect the velocity of longitudinal wave decreases in some direction of propagation (see Fig. 5(a)). Fig. 5(c) and (d) show that velocities of transversal waves decrease considerably for all directions of propagations **n** in contrast to the effect of deformation observed in the nearly incompressible materials (Fig. 5(a), (c) and (d)). The influence of stiffening on elastic wave propagation is rather weak in the case of auxetics as compared to nearly incompressible and highly compressible materials; yet it can be observed. In particular, phase velocity of transversal wave decreases more under compression when stiffening effect is pronounced (compare

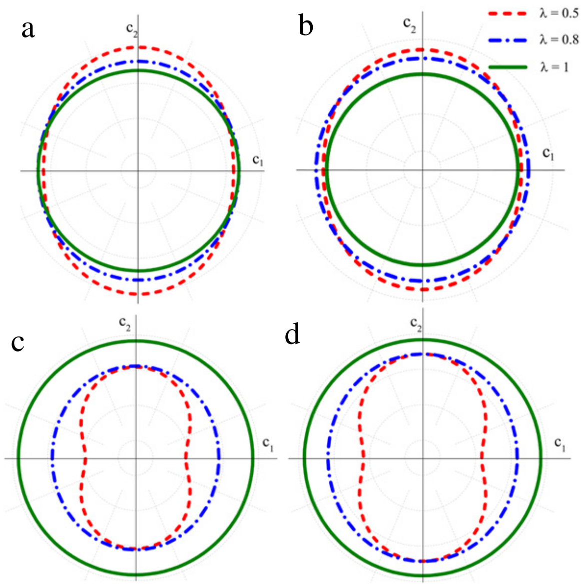

Fig. 5. Polar diagrams of the phase velocities in auxetics: for the quasi-longitudinal (a) and purely transversal (c) waves in Gent material with $J_m = 3$ and $K/\mu = -0.3$; for the purely longitudinal (b) and transversal (d) waves in neo-Hookean material with $K/\mu = -0.3$.

Fig. 5(c) vs (d)). The polar diagram of the phase velocity for the quasi-transversal wave in Gent material with $J_m = 3$ and $K/\mu = -0.3$ is similar to one plotted in Fig. 5(c), and is not shown here.

4. Concluding remarks

We derived explicit expressions for phase velocity for finitely deformed materials with pronounced stiffening effect and demonstrated the significant role of the deformation on elastic wave propagation on examples for nearly incompressible, highly compressible and extreme auxetic materials. Furthermore, we demonstrated how direction of wave propagation influences on the phase velocities of elastic waves. These findings may guide further design of mechanotunable acoustic metamaterials and phononic crystals with a large range of constituent properties. The local strain field in these engineered materials could be used to induce regions with extremely varied phononic properties to give rise to various acoustic effects. This opens a very rich and broad research avenue for designing tunable acoustic/phononic metamaterials.

Appendix A. Isomers of a fourth-rank tensor

Here we follow the notation of isomer firstly introduced by Ryzhak [34,35]. Let $\mathcal{M}$ be a fourth-rank tensor with the following representation as the sum of a certain number of tetrads:

$$\mathcal{M} = \mathbf{a}_1 \otimes \mathbf{a}_2 \otimes \mathbf{a}_3 \otimes \mathbf{a}_4 + \mathbf{b}_1 \otimes \mathbf{b}_2 \otimes \mathbf{b}_3 \otimes \mathbf{b}_4 + \cdots. \quad \text{(A.1)}$$

Let $(ijks)$ be some permutation of the numbers (1234). Then the isomer $\mathcal{M}^{(ijks)}$ is defined to be the fourth-rank tensor determined by the relation

$$\mathcal{M} = \mathbf{a}_i \otimes \mathbf{a}_j \otimes \mathbf{a}_k \otimes \mathbf{a}_s + \mathbf{b}_i \otimes \mathbf{b}_j \otimes \mathbf{b}_k \otimes \mathbf{b}_s + \cdots. \quad \text{(A.2)}$$

The fact that the isomer is independent of the choice of the polyadic representation of the original tensor can be readily proved by using well-known isomorphism between tensors and multilinear forms of the same rank.

Appendix B. Proof of absence of pure modes in general case in deformed Gent material

For clarity sake let us write an expanded form of tensor $\mathbf{n} \otimes \mathbf{n} : \mathbf{B} \otimes \mathbf{B}^{(1324)}$ and its scalar product on $\mathbf{n}$. First, let us write $\mathbf{B}$ and $\mathbf{B} \otimes \mathbf{B}$:

$$\mathbf{B} = \mathbf{F} \cdot \mathbf{F}^T = \lambda_1^2 \mathbf{e}_1 \otimes \mathbf{e}_1 + \lambda_2^2 \mathbf{e}_2 \otimes \mathbf{e}_2 + \lambda_3^2 \mathbf{e}_3 \otimes \mathbf{e}_3 \quad \text{(B.1)}$$

$$\begin{aligned}\mathbf{B} \otimes \mathbf{B} = {} & \lambda_1^4 \mathbf{e}_1 \otimes \mathbf{e}_1 \otimes \mathbf{e}_1 \otimes \mathbf{e}_1 + \lambda_2^4 \mathbf{e}_2 \otimes \mathbf{e}_2 \otimes \mathbf{e}_2 \otimes \mathbf{e}_2 \\ & + \lambda_3^4 \mathbf{e}_3 \otimes \mathbf{e}_3 \otimes \mathbf{e}_3 \otimes \mathbf{e}_3 \\ & + \lambda_1^2\lambda_2^2 \left(\mathbf{e}_1 \otimes \mathbf{e}_1 \otimes \mathbf{e}_2 \otimes \mathbf{e}_2 + \mathbf{e}_2 \otimes \mathbf{e}_2 \otimes \mathbf{e}_1 \otimes \mathbf{e}_1\right) \\ & + \lambda_1^2\lambda_3^2 \left(\mathbf{e}_1 \otimes \mathbf{e}_1 \otimes \mathbf{e}_3 \otimes \mathbf{e}_3 + \mathbf{e}_3 \otimes \mathbf{e}_3 \otimes \mathbf{e}_1 \otimes \mathbf{e}_1\right) \\ & + \lambda_2^2\lambda_3^2 \left(\mathbf{e}_2 \otimes \mathbf{e}_2 \otimes \mathbf{e}_3 \otimes \mathbf{e}_3 + \mathbf{e}_3 \otimes \mathbf{e}_3 \otimes \mathbf{e}_2 \otimes \mathbf{e}_2\right). \quad \text{(B.2)}\end{aligned}$$

Now we can write the isomer (1324) of fourth-rank tensor $\mathbf{B} \otimes \mathbf{B}$ as

$$\begin{aligned}\mathbf{B} \otimes \mathbf{B}^{(1324)} = {} & \lambda_1^4 \mathbf{e}_1 \otimes \mathbf{e}_1 \otimes \mathbf{e}_1 \otimes \mathbf{e}_1 \\ & + \lambda_2^4 \mathbf{e}_2 \otimes \mathbf{e}_2 \otimes \mathbf{e}_2 \otimes \mathbf{e}_2 + \lambda_3^4 \mathbf{e}_3 \otimes \mathbf{e}_3 \otimes \mathbf{e}_3 \otimes \mathbf{e}_3 \\ & + \lambda_1^2\lambda_2^2 \left(\mathbf{e}_1 \otimes \mathbf{e}_2 \otimes \mathbf{e}_1 \otimes \mathbf{e}_2 + \mathbf{e}_2 \otimes \mathbf{e}_1 \otimes \mathbf{e}_2 \otimes \mathbf{e}_1\right) \\ & + \lambda_1^2\lambda_3^2 \left(\mathbf{e}_1 \otimes \mathbf{e}_3 \otimes \mathbf{e}_1 \otimes \mathbf{e}_3 + \mathbf{e}_3 \otimes \mathbf{e}_1 \otimes \mathbf{e}_3 \otimes \mathbf{e}_1\right) \\ & + \lambda_2^2\lambda_3^2 \left(\mathbf{e}_2 \otimes \mathbf{e}_3 \otimes \mathbf{e}_2 \otimes \mathbf{e}_3 + \mathbf{e}_3 \otimes \mathbf{e}_2 \otimes \mathbf{e}_3 \otimes \mathbf{e}_2\right). \quad \text{(B.3)}\end{aligned}$$

Resolving $\mathbf{n}$ on the orthonormal basis $\mathbf{n} = n_1\mathbf{e}_1 + n_2\mathbf{e}_2 + n_3\mathbf{e}_3$, we obtain

$$\begin{aligned}\mathbf{n} \otimes \mathbf{n} : \mathbf{B} \otimes \mathbf{B}^{(1324)} = {} & \lambda_1^4 n_1^2 \mathbf{e}_1 \otimes \mathbf{e}_1 + \lambda_2^4 n_2^2 \mathbf{e}_2 \otimes \mathbf{e}_2 \\ & + \lambda_3^4 n_3^2 \mathbf{e}_3 \otimes \mathbf{e}_3 + \lambda_1^2\lambda_2^2 n_1 n_2 \left(\mathbf{e}_1 \otimes \mathbf{e}_2 + \mathbf{e}_2 \otimes \mathbf{e}_1\right) \\ & + \lambda_1^2\lambda_3^2 n_1 n_3 \left(\mathbf{e}_1 \otimes \mathbf{e}_3 + \mathbf{e}_3 \otimes \mathbf{e}_1\right) \\ & + \lambda_2^2\lambda_3^2 n_2 n_3 \left(\mathbf{e}_2 \otimes \mathbf{e}_3 + \mathbf{e}_3 \otimes \mathbf{e}_2\right) \quad \text{(B.4)}\end{aligned}$$

and

$$\begin{aligned}\mathbf{n} \otimes \mathbf{n} : \mathbf{B} \otimes \mathbf{B}^{(1324)} \cdot \mathbf{n} = {} & \left(\lambda_1^2 n_1^2 + \lambda_2^2 n_2^2 + \lambda_3^2 n_3^2\right) \\ & \times \left(\lambda_1^2 n_1 \mathbf{e}_1 + \lambda_2^2 n_2 \mathbf{e}_2 + \lambda_3^2 n_3 \mathbf{e}_3\right). \quad \text{(B.5)}\end{aligned}$$

Now, let $\mathbf{g}$ be a polarization vector, hence if $\mathbf{g} \parallel \mathbf{n}$ we have longitudinal polarization and if $\mathbf{g} \perp \mathbf{n}$ we have transversal polarization. Firstly, assume that $\mathbf{g} \parallel \mathbf{n}$ then expression (4) yields

$$\begin{aligned}\mathbf{Q}(\mathbf{n}) \cdot \mathbf{n} = {} & (\alpha + \beta\xi(\mathbf{n} \cdot \mathbf{B} \cdot \mathbf{n}))\,\mathbf{n} \\ & + 2\beta \left(\mathbf{n} \otimes \mathbf{n} : \mathbf{B} \otimes \mathbf{B}^{(1324)}\right) \cdot \mathbf{n}, \quad \text{(B.6)}\end{aligned}$$

where for convenience we denoted $\alpha = \frac{\mu}{J}\left(1 + \left(\frac{K}{\mu} - \frac{2}{3} - \frac{2}{J_m}\right)J^2\right)$ and $\beta = \frac{\mu J_m}{J\xi^2}$. Since in general case vector $\left(\mathbf{n} \otimes \mathbf{n} : \mathbf{B} \otimes \mathbf{B}^{(1324)} \cdot \mathbf{n}\right)$ is not collinear to $\mathbf{n}$ (see Eq. (B.5)), therefore vector $\mathbf{g} = \mathbf{n}$ is not an eigenvector of acoustic tensor, i.e. longitudinal polarization is absent, *q.e.d.*

Now let us assume that $\mathbf{g} \perp \mathbf{n}$ then (4) yields

$$\begin{aligned}\mathbf{Q}(\mathbf{n}) \cdot \mathbf{g} = {} & \beta\xi(\mathbf{n} \cdot \mathbf{B} \cdot \mathbf{n})\mathbf{g} \\ & + 2\beta \left(\mathbf{n} \otimes \mathbf{n} : \mathbf{B} \otimes \mathbf{B}^{(1324)}\right) \cdot \mathbf{g}, \quad \text{(B.7)}\end{aligned}$$

Suppose that $\mathbf{g}$ is an eigenvector of acoustic tensor then

$$\beta\xi(\mathbf{n}\cdot\mathbf{B}\cdot\mathbf{n})\mathbf{g}+2\beta\left(\mathbf{n}\otimes\mathbf{n}:\mathbf{B}\otimes\mathbf{B}^{(1324)}\right)\cdot\mathbf{g}=\theta\mathbf{g}. \quad \text{(B.8)}$$

Scalar multiplication of the last equation by $\mathbf{n}$ yields

$$\mathbf{n}\cdot\left(\mathbf{n}\otimes\mathbf{n}:\mathbf{B}\otimes\mathbf{B}^{(1324)}\right)\cdot\mathbf{g}=0$$

$$\text{or}\quad \left(\lambda_1^2 n_1\mathbf{e}_1+\lambda_2^2 n_2\mathbf{e}_2+\lambda_3^2 n_3\mathbf{e}_3\right)\cdot\mathbf{g}=0. \quad \text{(B.9)}$$

Yet last expression does not hold true in the general case. Consequently, $\mathbf{g}\perp\mathbf{n}$ is not an eigenvector of acoustic tensor, *q.e.d.*

References

[1] M. Biot, The influence of initial stress on elastic waves, J. Appl. Phys. 11 (1940) 522.
[2] C. Truesdell, W. Noll, in: S.S. Antman (Ed.), The Non-Linear Field Theories of Mechanics, third ed., Springer, 1965.
[3] A. Norris, Propagation of plane waves in a pre-stressed elastic medium, J. Acoust. Soc. Am. 74 (1983) 1642.
[4] R. Ogden, Non-Linear Elastic Deformations, Dover Publications, 1984.
[5] F. John, Plane elastic waves of finite amplitude. Hadamard materials and harmonic materials, Comm. Pure Appl. Math. 19 (1966) 309–341.
[6] M.S. Kushwaha, P. Halevi, L. Dobrzynski, B. Djafari-Rouhani, Acoustic band structure of periodic elastic composites, Phys. Rev. Lett. 71 (1993) 2022.
[7] V.K. Ignatovich, L.T.N. Phan, Those wonderful elastic waves, Amer. J. Phys. 77 (2009) 1162.
[8] R. Ogden, B. Sighn, Propagation of waves in an incompressible transversally isotripic elastic solid with initial stress: Biot revisited, J. Mech. Mater. Struct. 6 (2011) 453–477.
[9] M. Shams, M. Destrade, R. Ogden, Initial stresses in elastic solids: Constitutive laws and acoustoelasticity, Wave Motion 48 (2011) 552–567.
[10] W. Parnell, A.N. Norris, T. Shearer, Employing pre-stress to generate finite cloaks for antiplane elastic waves, Appl. Phys. Lett. 100 (2012) 171907.
[11] M. Destrade, R.W. Ogden, On stress-dependent elastic moduli and wave speeds, J. of Appl. Math. 78 (2013) 965–997.
[12] M. Hussein, M. Leamy, M. Ruzzene, Dynamics of phononic materials and structures: Historical origins, recent progress and future outlook, Appl. Mech. Rev. 66 (2014) 040802.
[13] P. Boulanger, M. Hayes, C. Trimarco, Finite-amplitude plane waves in deformed hadamard elastic materials, Geophys. J. Int. 118 (1994) 447–458.
[14] S. Shan, S.H. Kang, P. Wang, C. Qu, S. Shian, E.R. Chen, K. Bertoldi, Harnessing multiple folding mechanisms in soft periodic structures for tunable control of elastic waves, Adv. Funct. Mater. 24 (2014) 4935–4942.
[15] A. Bergamini, T. Delpero, L.D. Simoni, L.D. Lillo, M. Ruzzene, P. Ermanni, Phononic crystal with adaptive connectivity, Adv. Mater 26 (2014) 1343–1347.
[16] P. Boulanger, M. Hayes, Finite-amplitude waves in deformed mooney-rivlin materials, Q. J. Mech. Appl. Math. 45 (1992) 575–593.
[17] X. Zhuang, Y. Mai, D. Wu, F. Zhang, X. Feng, Two-dimensional soft nanomaterials: A fascinating world of materials, Adv. Mater. 27 (2015) 403–427.
[18] Y. Li, N. Kaynia, S. Rudykh, M. Boyce, Wrinkling of interfacial layers in stratified composites, Adv. Energy Mater. 15 (2013) 921–926.
[19] P. Wang, F. Casadei, S. Shan, J.C. Weaver, K. Bertoldi, Harnessing buckling to design tunable locally resonant acoustic metamaterials, Phys. Rev. Lett. 113 (2014) 014301.
[20] S. Zhang, C. Xia, N. Fang, Broadband acoustic cloak for ultrasound waves, Phys. Rev. Lett. 106 (2011) 024301.
[21] K. Bertoldi, M.C. Boyce, Wave propagation and instabilities in monolithic and periodically structured elastomeric materials undergoing large deformations, Phys. Rev. B 78 (2008) 184107.
[22] S. Rudykh, M. Boyce, Transforming wave propagation in layered media via instability-induced interfacial wrinkling, Phys. Rev. Lett. 112 (2014) 034301.
[23] Z. Chang, H.-Y. Guo, B. Li, X.-Q. Feng, Disentangling longitudinal and shear elastic waves by neo-hookean soft devices, Appl. Phys. Lett. 106 (2015) 161903.
[24] J.L. Williams, J.L. Lewis, Properties and an anisotropic model of cancellous bone from the proximal tibial epiphysis, Trans. ASME, J. Biomech. Eng. 104 (1982) 5–56.
[25] K.E. Evans, K.L. Alderson, Auxetic materials: the positive side of being negative, Eng. Sci. Educ. J. 9 (2000) 148–154.
[26] B.D. Caddock, K.E. Evans, Negative Poisson ratios and strain-dependent mechanical properties in arterial prostheses, Biomaterials 16 (1995) 1109–1115.
[27] S. Babaee, J. Shim, J. Weaver, E. Chen, N. Patel, K. Bertoldi, 3d soft metamaterials with negative Poisson ratio, Adv. Mater. 25 (2013) 5044–5049.
[28] P. Wang, J. Shim, K. Bertoldi, Effects of geometric and material nonlinearities on the tunable response of phononic crystals, Phys. Rev. B 88 (2013) 014304.
[29] P.I. Galich, S. Rudykh, Comment on "Disentangling longitudinal and shear elastic waves by neo-hookean soft devices", 2015.
[30] E. Arruda, M. Boyce, A three-dimensional constitutive model for the large stretch behavior of rubber elastic materials, J. Mech. Phys. Solids 41 (1993) 389–412.
[31] A.N. Gent, A new constitutive relation for rubber, Rubber Chem. Technol. 69 (1996) 59–61.
[32] C. Horgan, The remarkable gent constitutive model for hyperelastic materials, Int. J. Non-Linear Mech. 68 (2015) 9–16.
[33] M. Boyce, E. Arruda, Constitutive models of rubber elasticity: A review, Rubber Chem. Technol. 73 (2000) 504–523.
[34] E. Ryzhak, On stable deformation of unstable materials in a rigid triaxial testing mashine, J. Mech. Phys. Solids 41 (1993) 1345–1356.
[35] L. Nikitin, E. Ryzhak, On stability and instability of a compressed block pressed to a smooth basement, Mech. Solids 43 (2008) 558–570.
[36] Y. Wang, R. Lakes, Composites with inclusions of negative bulk modulus: Extreme damping and negative Poisson ratio, J. Compos. Mater. 39 (2005) 1645–1657.
[37] N. Gaspar, C.W. Smith, K.E. Evans, Effect of heterogeneity on the elastic properties of auxetic materials, J. Appl. Phys. 94 (2003) 6143.
[38] B. Auld, Acoustic Fields and Waves in Solids, Krieger publishing company, 1990.
[39] A. Nayfeh, Wave Propagation in Layered Anisotropic Media with Applications to Composites, Elsevier Science, 1995.
[40] N. Scott, The slowness surfaces of incompressible and nearly incompressible elastic materials, J. Elasticity 16 (1986) 239–250.
[41] G. Rogerson, N. Scott, Wave propagation in singly-constrained and nearly-constrained elastic materials, Q. J. Mech. Appl. Math. 45 (1992) 77–99.
[42] L. Chen, C. Liu, J. Wang, W. Zhang, C. Hu, S. Fan, Auxetic materials with large negative Poisson ratios based on highly oriented carbon nanotube structures, Appl. Phys. Lett. 94 (2009) 253111.
[43] K. Bertoldi, P. Reis, S. Willshaw, T. Mullin, Negative Poisson ratio behavior induced by an elastic instability, Adv. Mater. 22 (2010) 361–366.
[44] T. Still, M. Oudich, G.K. Auerhammer, D. Vlassopoulos, B. Djafari-Rouhani, G. Fytas, P. Sheng, Soft silicone rubber in phononic structures: Correct elastic moduli, Phys. Rev. B 88 (2013) 094102.
[45] P.J. Beltramo, D. Schneider, G. Fytas, E.M. Furst, Anisotropic hypersonic phonon propagation in films of aligned ellipsoids, Phys. Rev. Lett. 113 (2014) 205503.